Stellar Coronae with *XMM-Newton* RGS

M. Audard, M. Güdel

Paul Scherrer Institut, Würenlingen and Villigen, CH-5232 Villigen PSI, Switzerland,
audard@astro.phys.ethz.ch

R. Mewe, A. J. J. Raassen

Space Research Organization of the Netherlands, Sorbonnelaan 2, 3584 CA Utrecht, The Netherlands

E. Behar

Columbia Astrophysics Laboratory, Columbia University, 550 West 120th Street, New York, NY 10027, USA

Abstract

First results from high-resolution coronal spectroscopy with the Reflection Grating Spectrometers on board the *XMM-Newton* satellite are reviewed. This paper is structured in two sections: The first section presents results in the context of coronal structure of active stars, while the second discusses X-ray variability in these stars.

1. Introduction

High-resolution X-ray spectroscopy now available from *Chandra* and *XMM-Newton* can measure, for the first time, densities, elemental abundances, the thermal structure, and mass motions fror a large number of coronal sources based on atomic line diagnostics in the X-ray regime. Such measurements are pivotal for our understanding of coronal structure, coronal heating, and mass transfer from the lower layers into the hot corona.

Additionally, stellar coronae often display variability in their X-ray emission. Energetic explosive events (flares), eclipses, and rotational modulation are among the most interesting features found in X-ray light curves of coronal stars. Flares are at the center of a scenario that assumes an ensemble of flares as agents of heating of stellar coronae ("microflare hypothesis"; e.g., Parker 1988). Recent results suggest that flares can contribute significantly to the coronal heating of active stars (Audard et al. 2000). In a standard model, magnetic energy is released during a flare, heating the dense layers of chromospheric material. Hot ionised material is then driven into the corona by the pressure increase and fills the coronal loops (chromospheric evaporation; see Antonucci et al. 1994). Optically thin X-ray radiation occurs through continuum processes and electronic transitions.

Flares are therefore important agents that bring "fresh" material from the chromospheric layers to the corona. In the non-flaring Sun, a First Ionization Potential (FIP) effect is observed, with enhanced coronal abundances for elements with low FIP (< 10 eV), while high-FIP elements show solar photospheric values. In the stellar case, evidence for the presence of the FIP effect is less clear, but has been found in some stars (e.g., Drake et al. 1995,1997). Recently, Brinkman et al. (2001) has found in HR 1099 evidence for an *inverse*

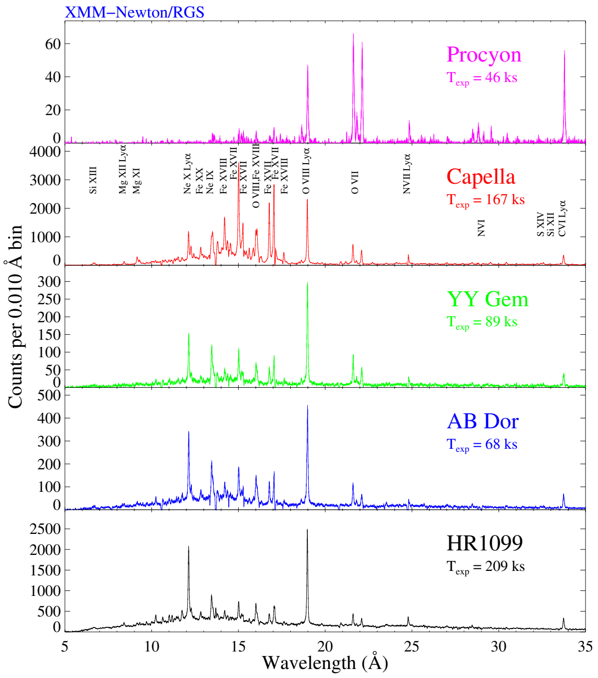

Fig. 1.— Five spectra observed with RGS, smoothed to 30 mÅ effective resolution. The average coronal temperature increases from Procyon (top), to Capella (2nd panel), YY Gem (3rd panel), AB Dor (4th panel) and HR 1099 (bottom).

FIP effect and strong enhancement of Ne relative to O. Stellar coronal flares often show enhanced metal abundances (e.g., Ottmann & Schmitt 1996). Also, some classes of solar flares can be Ca-rich (Ca is a low-FIP element; Sylwester et al. 1984) or Ne and S-rich (Ne and S are high-FIP elements; Schmelz 1993).

The two Reflection Grating Spectrometers on board *XMM-Newton* observed HR 1099 as their First Light target and later continued to obtain deep X-ray spectra of various coronal sources for an extended survey of coronal activity. In this paper, we report a first summary of results on coronal structure (Sct. 2) and on X-ray variability (Sct. 3) of active stars.

2. Coronal Structure

2.1. RGS Spectra and Thermal Structure

Stars of higher activity level reveal coronae of higher average temperature. This simple correlation (see, e.g., Güdel, Guinan, & Skinner 1997) has defied a conclusive physical explanation, although models involving a higher average but quiescent heating rate (Schrijver, Mewe, & Walter 1984) or higher "micro"-flare rate (Güdel et al. 1997) have been discussed in the literature.

RGS spectroscopy explicitly reveals differences in the thermal structure through atomic lines. Figure 1 shows spectra of five sources (Procyon, Capella, YY Gem, AB Dor, and HR 1099 in order of increasing "activity" or average temperature). The increasing relative importance of the continuum toward higher activ-

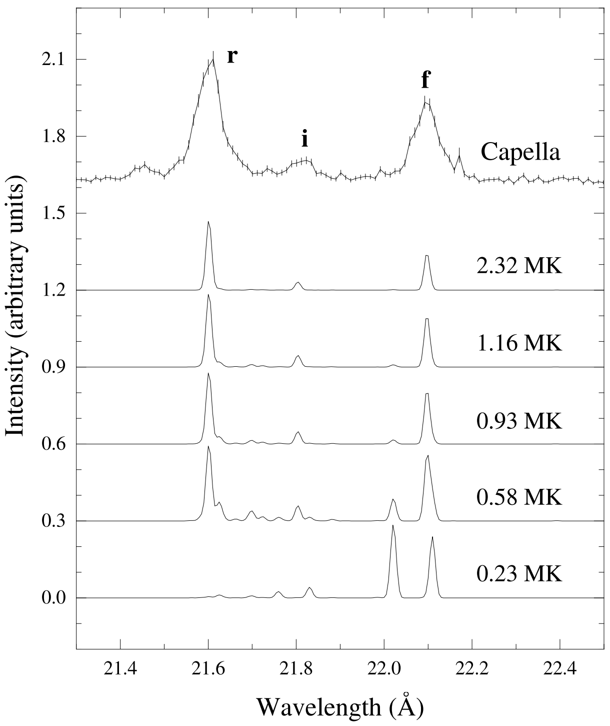

Fig. 2.— Observed O VII triplet in Capella's spectrum with calculated spectra of the O VII and O VI DR satellite lines for five different electron temperatures. The plots are normalised to the strongest line in each spectrum. Note the steep temperature sensitivity of the DR satellites (Audard et al. 2001b)

ity is evident (note that much of Capella's "pseudo-continuum" around 15 Å is due to overlapping scattering line wings). The rather cool "solar-like" corona of Procyon reveals only weak Fe lines, while the spectrum is dominated by lines of C V, N VI, N VII, and O VII, formed around 1–3 MK. A further evident temperature diagnostic is given by the flux ratio between the O VIII Lyα line at 18.97 Å and the O VII resonance line at 21.6 Å; clearly, this ratio systematically increases from Procyon to HR 1099. The EM at the coolest (< 1 MK) temperatures can be constrained using dielectronic recombination satellite lines of O VI (Fig. 2; Audard et al. 2001b).

2.2. Elemental Abundances

Coronal elemental abundances are known to deviate from photospheric abundances in the Sun (Meyer 1985; Feldman et al. 1992) such that elements with a low FIP (below 10 eV) are overabundant by an average factor of $\approx$4 (Feldman et al. 1992). Various scenarii for the related fractionation process have been proposed, involving magnetic and electric fields (e.g., Hénoux 1995 for a review). However, coronal abundances of *active* stars do not show evidence for clear FIP dependencies but rather indicate that most elements are *depleted* in the corona (Antunes et al. 1994; Drake 1996; White 1996).

Elemental abundances can now unambiguously be determined from separated lines in the X-rays. Fig. 3 shows the surprising result (Brinkman et al. 2001) from the RGS spectrum of HR 1099 (Fig. 1): the relative abundances (normalised to oxygen) *increase* with increasing FIP, in a nearly exponential fashion, with Ne showing an unusually high abundance evident in the very strong Ne X line at 12.1 Å in Fig 1. There is as of yet no consistent model for this *inverse FIP effect*, but Brinkman et al. (2001) suggest that mechanisms analogous to solar Ne- and S-rich flares may enrich the corona with high-FIP species. Similar results are reported for the other two active sources AB Dor and YY Gem (Güdel et al. 2001ab).

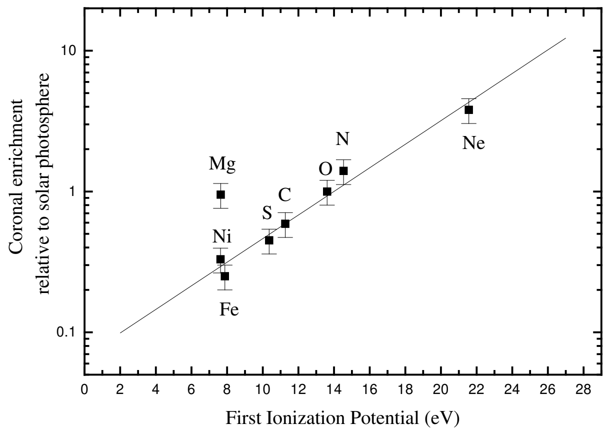

Fig. 3.— Abundances derived for HR 1099 from *XMM-Newton* RGS data, relative to solar photospheric, as a function of FIP and normalised to the oxygen abundance. Note inverse FIP effect (Brinkman et al. 2001).

2.3. Geometric Structure and Densities

X-ray coronal structure is inferred indirectly, based on eclipse mapping, rotational modulation, or density measurements. The latter approach is available in the RGS range based on the He-like density-sensitive triplets of N VI, O VII, Ne IX, Mg XI, and Si XIII. Fig. 9 shows an example of the O VII triplet of the quiescent AB Dor. Best-fit measurements indicate a density of $(3 \pm 1.5) \times 10^{10}$ cm^{-3}, quite high by solar standards

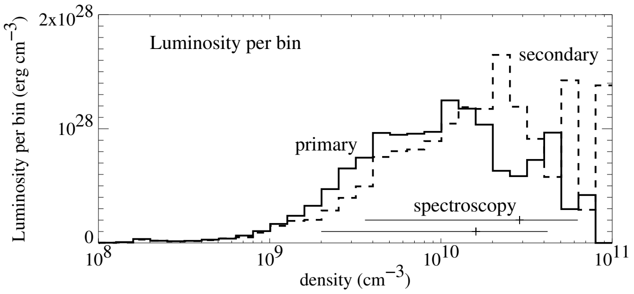

Fig. 4.— Coronal modeling from light curve inversion of the eclipsing binary YY Gem. Luminosity contribution as a function of density. The bars at the bottom indicate the spectroscopically measured electron densities from RGS data (two methods, see Güdel et al. 2001b).

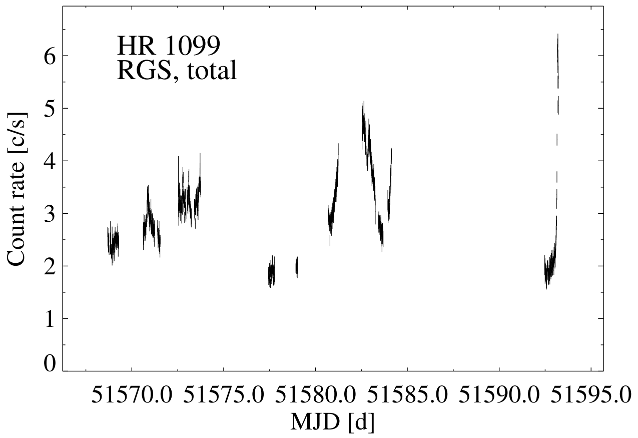

Fig. 5.— Total 1st and 2nd order RGS light curve of HR 1099 (Audard et al. 2001a).

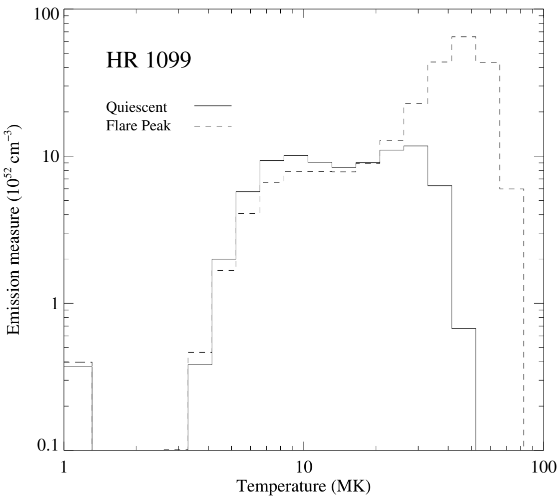

Fig. 6.— Realisations of the quiescent (solid) and flare peak (dash) EM distributions for HR 1099 using Chebychev polynomials of order 6 (Audard et al. 2001a).

(but possible in solar active regions). This density value refers to relatively cool material (T of a few MK). However, heavier elements such as Mg tentatively indicate much higher densities for hotter material, up to the order of 10^{12} cm^{-3} (Audard et al. 2001b for Capella). This bi-modal distribution of densities (cool material at low densities, hot material at higher densities) suggests the presence of separate loop structures, with low-lying, compact hot loops on the one hand and larger, cooler loops on the other hand (Mewe et al. 2001).

Mutual eclipses in binary systems can be used to infer the geometry of the X-ray corona. The dM1e active binary system YY Gem was extensively observed by *XMM-Newton* (Güdel et al. 2001b), including three deep eclipses. The eclipse light curves were used to reconstruct realisations of fitting geometric coronal models. It was found that the plasma is required to be relatively close to the star, with an average density scale height of $(1-4)\times10^{10}$ cm, which agrees very well with the spectroscopically measured T of 3$-$10 MK. Most of the detected X-ray light is then emitted from densities around several times 10^9 cm^{-3} to a few times 10^{10} cm^{-3} (Fig. 4), and these values are again in agreement with spectroscopic results.

3. X-ray Variability

3.1. X-ray Rotational Modulation in HR 1099

The RGS observed the RS CVn binary system HR 1099 for a time span of about 25 days (Fig. 5). The light curve shows variability on short and long time scales. Similar to previous results (Agrawal & Vaidya 1988; Drake et al. 1994), rotational modulation is suggested, with maximum flux when the more active star (K1 IV) is in front. Recently, Ayres et al. (2001) found consistency between line wavelength shifts and the orbital motion of the K component of HR 1099. Taken together, these observations suggest that one or several active regions are present on the hemisphere of the K star that is facing away from its companion (Audard, Güdel, & Mewe 2001a).

3.2. RGS Spectra of Flares

Time-dependent spectroscopy has been performed on the flare data sets (HR 1099, AB Dor, YY Gem). We have first studied the quiescent emission measure (EM) distribution and found it to be continuous over a wide range of temperatures (e.g., Fig. 6). The EM drops to low values below ≈5 MK. A small but significant EM is needed around 1–3 MK in order to explain "cool" lines such as the bright C VI Lyα line and the O VII triplet around 22 Å. During the flare in HR 1099, the EM changes considerably but only at high temperatures while the cooler plasma remains essentially unchanged, indicating that the flare does not affect a major part of the corona. Above 30 MK, however, a significant EM component develops, with contributions from plasma up to about 90 MK (Fig. 6). During this strong heating, Fe XXIV lines become significantly enhanced. The rapid flares on AB Dor (Fig. 7) show

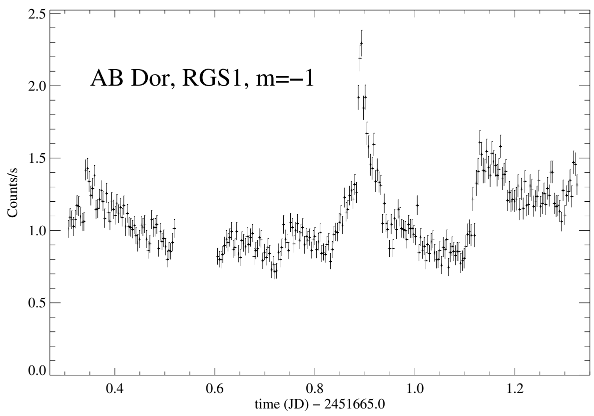

Fig. 7.— RGS1 first order light curve of AB Dor (April 30/May 1; Güdel et al. 2001a).

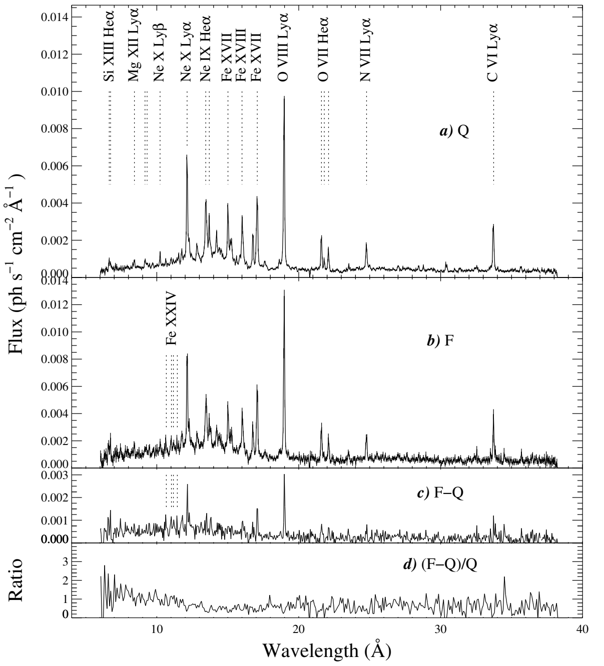

Fig. 8.— RGS fluxed spectrum of the **(a)** quiescent and **(b)** flaring AB Dor, **(c)** the difference spectrum, and **(d)** the ratio "(flare−quiescent)/quiescent". Data are binned to a resolution of 0.04375 Å for (a-c) and to 0.0875 Å for (d). Note different flux scales. The Fe XXIV lines and an excess continuum shortward of 10 Å are evident in (c) and (d) (Güdel et al. 2001a).

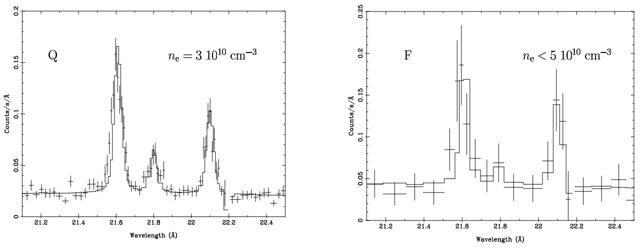

Fig. 9.— Density-sensitive line triplet of He-like O VII (resonance, intercombination, and forbidden line for increasing wavelength). Left panel shows best-fit (histogram) to RGS data (error bars) during AB Dor's quiescence, while right panel shows the triplet for data selected during flares (Güdel et al. 2001a).

similar spectral features: strong Fe XXIV lines become apparent during the flares, and the continuum becomes enhanced shortward of 12 Å (Fig. 8).

3.3. Variable Abundances

Elemental abundances vary significantly during the observed flares. The metal abundance during one of AB Dor's flare increases by a factor of ≈3 and decays back to its quiescent level (Güdel et al. 2001a). In HR 1099 flare spectra, the Fe and Si elemental abundances increase by factors ≈3, and 10 (despite large error bars, the latter abundance increases by a factor of 6 at minimum), respectively, while the Ne (high-FIP) abundance does *not* increase, staying constant at its quiescent level, within the confidence ranges (Audard et al. 2001a).

3.4. Densities

The He-like O VII triplet around 22 Å provides insight into the *average* density of the "cool" plasma component (around 1–3 MK). Significant quiescent densities have been found in AB Dor ($n_e = [3 \pm 1.5] \times 10^{10}$ cm^{-3}; Güdel et al. 2001a), YY Gem ($n_e = 1.6^{+2.6}_{-1.4} \times 10^{10}$ cm^{-3}; Güdel et al. 2001b), while only upper limits can be derived for HR 1099 ($< 1 \times 10^{10}$ cm^{-3}; Audard et al. 2001a) and Castor ($< 3 \times 10^{10}$ cm^{-3}; Güdel et al. 2001b). No appreciable change in the *average* density of the emitting *cooler* material has been found (Fig. 9) during flares. This indicates that the average density of the cooler material (1–3 MK) does not significantly increase during such flares. Recalling Fig. 6, it implies that the flares predominantly affect hot material and have limited influence on the EM of the relatively cool plasma.

4. Summary and Conclusions

Stellar coronae have been compared with scaled-up versions of the solar corona although this analogy has clearly become doubtful. Not only are the X-ray luminosities of active stars orders of magnitude larger than the Sun's, but the thermal structure is also very different, ranging from cooler solar-like structures of a few MK (probably analogous to the Procyon corona) up to *non-flaring* coronal components at 20−30 MK. Spectroscopy clearly provides the necessary information for further study.

The most crucial results from this early *XMM-Newton* RGS stellar coronal survey set active stars apart from the Sun. Coronal elemental abundances, although known before to deviate from solar behaviour, are now showing a clear systematic dependence on the FIP value, such that high-FIP elements (O, N, Ne) are largely overabundant compared to low-FIP elements (Fe, Mg, Si, Ni), thus defining an *inverse FIP effect*, contrary to the solar trends. The Sun does occasionally reveal Ne- and S-rich flares (i.e., high-FIP elements are enriched in the flaring plasma), and analogous processes may be responsible for the anomalously high Ne abundance seen in active stars.

Densities found so far for active stars are high for solar standards, even for relatively cool plasma. High densities in hot plasma, although still only marginally detected, have no solar analogy except for flares. Taken together, we speculate that the mechanisms for heating to high temperatures and for inverting the coronal abundance pattern are related and unknown to the *non-flaring* Sun.

Flares have also been found to be frequent in the stellar coronal sources observed by *XMM-Newton*. The presence of very hot (up to several tens of MK) material has been inferred, and evidence for elemental abundance enhancements has been found. Low-FIP elements appear to increase significantly during flares, while the high-FIP element Ne stays at constant abundance. This behaviour contrasts with the *inverse* FIP effect found in these coronae during quiescence. The flare EM distributions appear to be composed of a very hot plasma (up to 100 MK) that evolves rapidly, and of a stable quiescent plasma. This result is consistent with the absence of a change in the density of the cool material.

Stellar flares are important probes for stellar coronal plasma and the coronal heating mechanism. Our *XMM-Newton* observations indicate that flares are also important as agents that relate chromospheric / photospheric plasma with coronal plasma. The very high temperatures attained by these flares are unknown to solar flares. Such observations are important to extend solar knowledge to more extreme conditions appropriate for magnetically active stars.

The PSI group is supported by the Swiss Academy of Natural Sciences and the Swiss National Science Foundation (grants 2100-049343 and 2000-058827). SRON is financially supported by the Netherlands Organization for Scientific Research (NWO). The Columbia University team acknowledges generous support from the National Aeronautics and Space Administration. This work is based on observations obtained with XMM-Newton, an ESA science mission with instruments and contributions directly funded by ESA member states and the USA (NASA).

REFERENCES

Antonucci, E., Gabriel, A. H., & Dennis, B. R. 1984, ApJ, 287, 917

Antunes, A., Nagase, F., & White, N. E. 1994, ApJ, 436, L83

Audard, M., Güdel, M., & Mewe, R. 2001a, A&A, 365 (in press)

Audard, M., Güdel, M., Drake, J. J., & Kashyap, V. L. 2000, ApJ, 541, 396

Audard, M., Behar, E., Güdel, M., Raassen, A. J. J. et al. 2001b, A&A, 365, (in press)

Ayres, T. R., Brown, A., Osten, R. A. et al. 2001, ApJ, (in press)

Brinkman, A. C., Behar, E., Güdel, M. et al. 2001, A&A, 365 (in press)

Drake, J. J., Laming, J. M., & Widing, K. G. 1995, ApJ, 443, 393

Drake, J. J., Laming, J. M., & Widing, K. G. 1997, ApJ, 478, 403

Drake, S. A. 1996, in 6th Annual Astrophysics Conference, ed. S. S. Holt & G. Sonneborn (San Francisco: ASP), 215

Feldman, U., Mandelbaum, P., Seely, J.F., Doschek, G.A., & Gursky, H. 1992, ApJS, 81, 387

Güdel, M. 1997, ApJ, 480, 121

Güdel, M., Audard, M., Briggs, K. et al. 2001a, A&A, 365 (in press)

Güdel, M., Audard, M., Magee, H. et al. 2001b, A&A, 365 (in press)

Güdel, M., Guinan, E. F., & Skinner, S.L. 1997, ApJ, 483, 947

Hénoux, J.-C. 1995, Adv. Space Res., 15, 23

Mewe, R., Raassen, A. J. J., Drake, J. J. et al. 2001, A&A, submitted

Meyer, J.-P. 1985, ApJS, 57, 173

Ottmann, R., & Schmitt, J. H. M. M. 1996, A&A, 307, 813

Parker, E. N. 1988, ApJ, 330, 474

Schmelz, J. T. 1993, ApJ, 408, 373

Schrijver, C. J., Mewe, R., & Walter, F. M. 1984, A&A, 138, 258

Sylwester, J., Lemen, J. R., & Mewe, R. 1984, Nature, 310, 665

White, N. E. 1996, in 9th Workshop on Cool Stars, Stellar Systems, and the Sun, eds. R. Pallavicini and A. K. Dupree (San Francisco: ASP), 193